https://doi.org/10.15255/KUI.2026.009
KUI-41/2026
Original scientific paper
Received February 25, 2026
Accepted May 3, 2026

Experimental and Computational Modelling of Immune Response and Toxicological Assessment of Urban Nanoparticles in an Earthquake-Affected City

Y. Ermurat [a,b*]

This work is licensed under a Creative Commons Attribution 4.0 International License

[a] Department of Basic Sciences, Engineering Architecture and Design Faculty, Kahramanmaraş İstiklal University, 46 060 Kahramanmaraş, Turkey
[b] Engineering Faculty, Bolu Abant Izzet Baysal University, 14 030 Bolu, Turkey

Abstract

Urban nanoparticles (UNPs) generated in post-disaster environments represent complex and potentially hazardous components of urban pollution with significant implications for public health. This study investigates the physicochemical characteristics and potential biological implications of UNPs collected from the earthquake-affected city centre of Kahramanmaraş, Türkiye, following the February 2023 seismic events. Dust samples were analysed using transmission electron microscopy (TEM), which revealed a heterogeneous particle population ranging from 50 to 500 nm, including a significant ultrafine fraction (< 100 nm) with irregular and agglomerated morphologies. Energy-dispersive X-ray spectroscopy (EDX) identified dominant elements (O, C, Ca, Si) alongside transition metals such as Fe, Cr, and Cu, indicating mixed UNPs sources. Computational analyses highlighted notable compositional variability and inter-element relationships. Predictive modelling approaches were applied to assess potential nanotoxicological and immunological implications.

Machine-learning models demonstrated that toxicity was influenced by particle size, elemental composition, and exposure duration, with chromium and copper emerging as key contributors to oxidative stress. Markov chain and Monte Carlo simulations further revealed dynamic particle behaviour, bioaccumulation potential, and associated uncertainties over time. Integration of structural, compositional, and computational findings provides a comprehensive framework for understanding the nanoparticle-associated risks. Comparative evaluation with *in vivo* or *in vitro* experimental studies suggests potential outcomes including oxidative stress, inflammation, and immune dysregulation. These findings underscore the importance of multidisciplinary approaches for assessing environmental health risks in post-earthquake urban environments.

Keywords

Urban nanoparticles, experimental and computational modelling, transmission electron microscopy (TEM), immune responses, nanotoxicological effects

1 Introduction

Urban nanoparticles (UNPs) are an increasingly important class of airborne particulate pollutants originating from anthropogenic activities such as construction, industrial emissions, vehicular exhaust, and other ecological disturbances.[1–4] In recent years, natural disasters and post-disaster reconstruction processes have also emerged as significant contributors to urban particulate pollution due to large-scale structural damage, debris resuspension, and ongoing rebuilding activities.[5–8] These processes generate complex mixtures of fine and ultrafine particles that remain suspended in the atmosphere and contribute to deteriorating air quality in densely populated urban locations.[9–11]

Due to their nanoscale dimensions, typically below 100 nm for ultrafine fractions, urban nanoparticles exhibit high surface-area-to-volume ratios, enhanced reactivity, and the ability to remain airborne for extended periods.[12–15] These properties allow them to penetrate deep into the human respiratory tract, reaching alveolar regions and potentially entering systemic circulation.[16–18] Once internalised, nanoparticles may interact with biological systems, leading to oxidative stress, inflammatory responses, and cellular dysfunction.[19–22] The toxicological impact of these particles is strongly dependent on their physicochemical characteristics, including size, morphology, surface charge, and elemental composition.[23–26]

A substantial body of literature has demonstrated that particulate matter containing metal oxides, carbonaceous species, and mixed inorganic components can induce a range of adverse biological effects.[27–30] These include immune cell activation, reactive oxygen species (ROS) generation, mitochondrial dysfunction, and DNA damage.[31–34] Smaller particles are generally considered more biologically active due to their increased ability to cross cellular barriers and interact with intracellular components.[35–37] In particular, ultrafine particles have been associated with enhanced pulmonary deposition and systemic distribution compared to larger particulate fractions.[38–40]

The elemental composition of urban nanoparticles plays a critical role in determining their toxicological potential.[41–43] Metal-containing particles such as those enriched in iron (Fe), chromium (Cr), aluminium (Al), silicon (Si), copper (Cu), and titanium (Ti) have been widely reported to exhibit higher oxidative potential and greater capacity to induce inflammatory responses.[44–48] Transition metals such as iron and copper can catalyse redox reactions, leading to the production of reactive oxygen species,[49–51] while chro-

* Corresponding author: Yakup Ermurat, PhD
Email: yakupermurat@ibu.edu.tr

mium and aluminium compounds have been associated with genotoxic and immunomodulatory effects under certain exposure conditions.[52–55] Silicon-based particles, particularly in nanoform, have also been linked to pulmonary inflammation and cellular stress responses depending on particle size and surface characteristics.[56–59]

Engineered nanoparticles (ENPs) have been extensively studied under controlled laboratory conditions to understand their physicochemical behaviour and biological interactions.[60–63] These studies have provided valuable insights into size-dependent toxicity, surface reactivity, and cellular uptake mechanisms.[64–67] However, ENPs often differ significantly from locationally derived urban nanoparticles in terms of compositional complexity, heterogeneity, and source variability.[68–71] While ENP studies provide useful reference frameworks, direct extrapolation to real-world urban particle exposure remains limited due to these inherent differences.[72–74]

Urban nanoparticles, in contrast, represent complex particle mixtures formed under uncontrolled conditions.[75–77] They typically consist of heterogeneous aggregates containing mineral dust, combustion-derived carbonaceous particles, metallic fragments, and secondary atmospheric species.[78–81] This compositional complexity makes their characterisation more challenging but also more environmentally relevant.[82–84] Despite growing interest in nanoparticle toxicology, there remains a lack of detailed experimental studies focusing on real-world urban nanoparticles, particularly those generated under post-disaster conditions.[85–87]

Post-earthquake urban locations represent a particularly important yet underexplored source of nanoparticulate pollution.[88–90] Structural collapse, demolition activities, and reconstruction efforts contribute to the release and resuspension of fine particulate matter, significantly altering local air quality.[91–93] In such areas, populations may experience elevated exposure to complex particulate mixtures with uncertain health implications.[94–96] However, the physicochemical properties and potential toxicity of nanoparticles derived from such settings remain insufficiently characterised in the current literature.[97–99]

Given these challenges, there is a growing need for integrated approaches that combine advanced experimental techniques with data-driven analytical methods to better understand urban nanoparticle behaviour.[100–102] Transmission electron microscopy (TEM) provides high-resolution imaging capabilities that enable detailed characterisation of particle morphology, size distribution, and structural features at the nanoscale.[103–105] Complementary elemental analysis techniques allow identification of metallic and non-metallic components, offering insight into compositional variability and potential sources of toxicity.[106–108]

In addition to experimental characterisation, computational and machine-learning approaches have increasingly been applied in toxicological investigations.[109–111] Methods such as decision-tree analysis, random-forest modelling, k-means clustering, and artificial neural networks enable identification of patterns, classification of complex datasets, and exploration of nonlinear relationships between physicochemical properties and toxicity indicators.[112–113] These methods are particularly useful in systems where experimental data are heterogeneous and multifactorial in nature.[114]

2 Materials and methods

Urban dust samples containing particulate matter were collected from the city centre of Kahramanmaraş, Türkiye, following the February 2023 earthquake. Samples were obtained from surface dust deposits in open urban areas affected by structural damage and reconstruction activities. The dust samples were collected using clean, inert tools, and stored in sealed, contamination-free containers to form a representative blended material. No chemical or physical pre-treatment was applied prior to analysis in order to preserve the original locational characteristics of the particulate matter. A small amount of dry dust sample was directly deposited onto carbon-coated copper grids for microscopic analysis. Excess material was gently removed to ensure a thin, dispersed layer suitable for imaging. The prepared grids were air-dried under ambient laboratory conditions prior to analysis. Morphological and structural characterisation of the particles was performed using a JEOL transmission electron microscope (TEM) established in Çanakkale Onsekiz Mart University Science and Technology Application and Research Centre. The instrument was operated under standard imaging conditions appropriate for nanoscale resolution. TEM micrographs were used to examine particle morphology, aggregation state, and approximate size distribution. Particle dimensions were determined by measurement of representative particles directly from acquired TEM images. The elemental composition of selected particles was analysed using energy-dispersive X-ray spectroscopy (EDX) coupled with the TEM system. Spectra were collected from representative particle regions to identify major and minor elemental constituents. The resulting elemental data were used for qualitative and semi-quantitative assessment of compositional variability within the sampled urban dust nanoparticles. Elemental abundance data obtained from EDX analysis were organised into a structured dataset for statistical evaluation. Correlation analysis was performed to investigate relationships between detected elements within the samples. Results were visualised using correlation matrices and heatmaps to illustrate compositional associations.

Data visualisation was performed using Python and MATLAB computational tools. Heatmaps and graphical representations were generated to illustrate elemental relationships and compositional patterns. These analyses were used for exploratory interpretation of nanoparticle composition. Biological outcome modelling was not applied in this study.

3 Results

The urban nanoparticle (UNP) samples were analysed in their native, unprocessed state to preserve their original physicochemical characteristics. This approach ensured

that the measurements reflected authentic environmental particulate matter without laboratory alteration or post-processing effects. Microstructural analysis in the 50–500 nm range revealed a heterogeneous population of particles with irregular morphology, including angular, fragmented, and agglomerated structures. A significant fraction of particles was below 100 nm, corresponding to the ultrafine nanoparticle (UNP) fraction. The observed variability in particle size and shape indicated a mixed particulate system influenced by multiple formation sources.

Microscopic analysis of the powder sample revealed that the UNPs varied significantly in size, form, and shape, depending on their source and composition, as shown in Fig. 1. These NPs typically range from 50 to 500 nm in size, but particles smaller than 100 nm are classified as ultrafine UNPs, which are a common type of particulate matter. The size of these particles plays a key role in their environmental behaviour and potential impact on human health. Due to their small dimensions, ultrafine particles can penetrate deeply into the lungs and bloodstream, thereby posing severe health risks.

The elemental composition of UNPs provided important insight into their potential health impacts, revealing a chemically diverse mixture of elements present, as shown in Fig. 2. EDX spectroscopy coupled with TEM enabled qualitative and quantitative chemical analysis of the UNP samples. The EDX utilised high signal-to-noise ratios and rapid data collection to gather X-ray spectra from small sample volumes. This technique decisively quantified the elemental composition of the pollutants, including both inorganic and organic compounds in UNPs, thereby providing insight into possible pollution sources and potential health impacts. Extensive analysis identified several key elements, including O, C, Ca, Si, Fe, Al, Cr, Mg, together with less abundant elements like S, K, Sb, Cu, Ti, P, Mo, and Os. These elements contribute to the physical and chemical properties of the NPs, influencing their behaviour in urban environments. These findings demonstrate the complexity and diversity of the analysed particles, suggesting the potential for diverse immuno-toxicological effects. Oxygen and carbon were identified as the dominant elements, with oxygen concentrations ranging from 2.8 to 39.5 % and carbon contributing between 23.8 and 45.9 % of the total composition. Calcium was also present in significant amounts, varying from 7.7 to 42 %, reflecting its important role in the formation of certain NP types. Si was likewise prominent, with concentrations ranging from 0.6% to 15.4 %, further suggesting the present of diverse material sources. Other common elements included Fe (0.7–2.7 %), Al (0.2–4 %), Cr (0.4– 2.2 %), Mg (0.2–11.6 %), and S (0.2–0.7 %), all of which contribute to the overall toxicological profile of the NPs. Trace amounts of Sb, K, Cu, Ti, Os, and P were also detected, which, although present in lower concentrations, may still contribute to the adverse biological effects of UNPs, especially when considering their potential to accumulate in the body over time.



Fig. 1 – Microstructural TEM images of the particle sample obtained across a scale range of 50–500 nm. These images reveal the diverse shapes and sizes of the nanoparticles, indicating significant variability based on their origin and material composition.

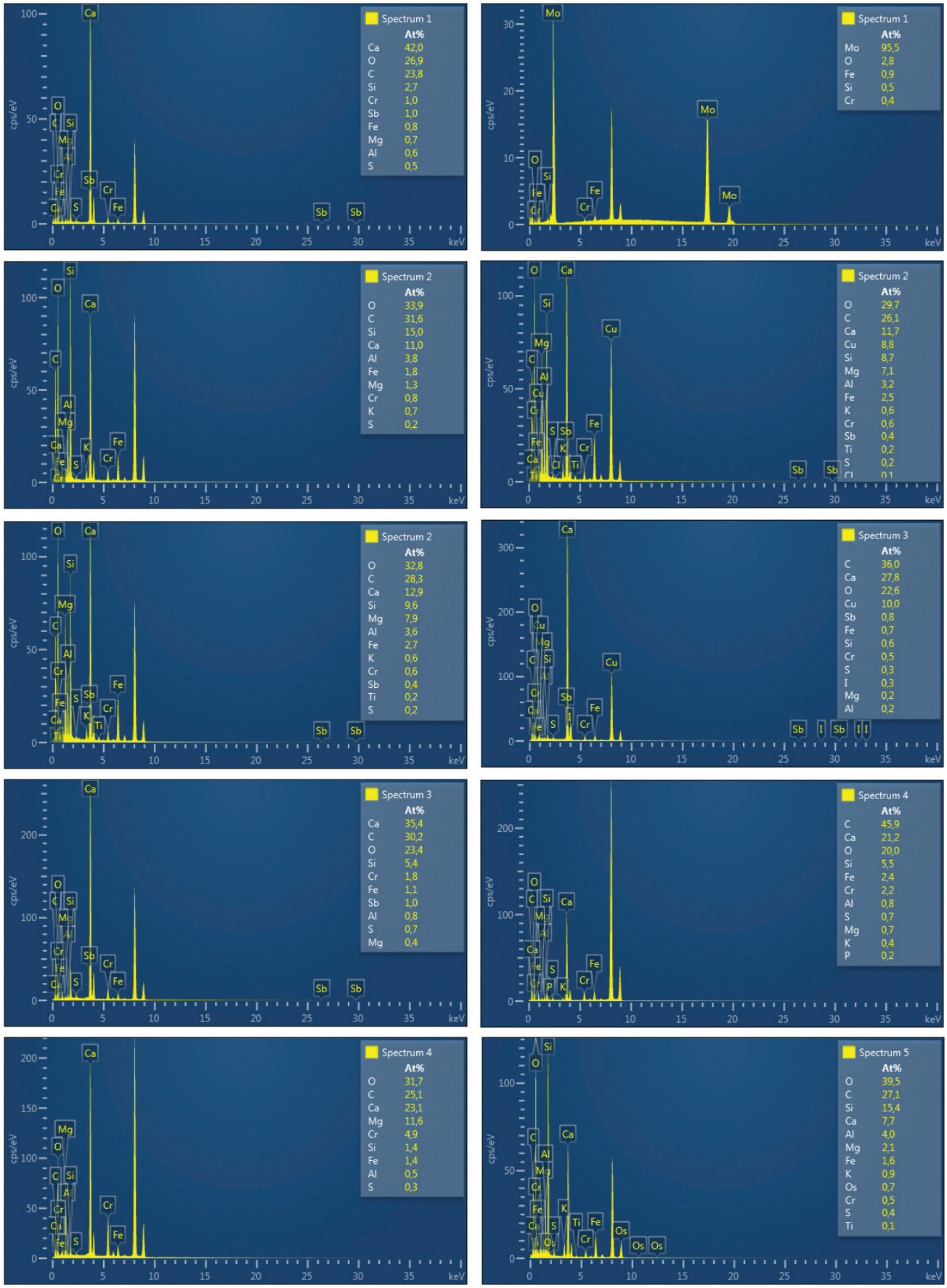


Fig. 2 – Energy-dispersive X-ray (EDX) spectroscopy peak patterns of the elemental constituents of UNPs, illustrating the elemental composition of the UNP samples

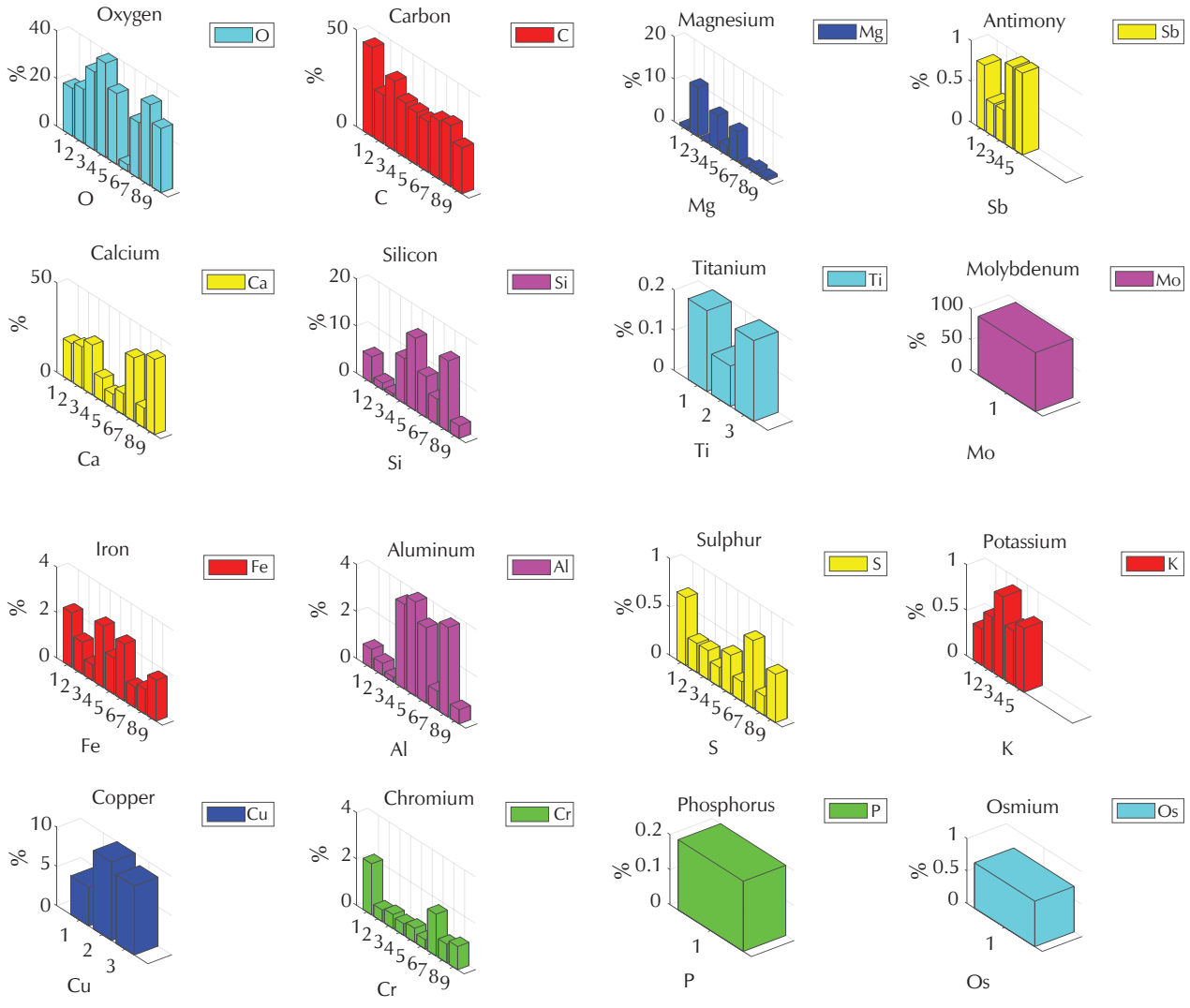


Fig. 3 – Percentage distribution of elements across multiple analyses, illustrating the prevalence of key components

As presented in Fig. 3, the percentage distribution of the elements detected across the analyses revealed the composition of NPs. Elements such as O, C, Ca, Si, Fe, Al, Cr, and Mg were identified as the predominant components across all analyses, playing essential roles in the physical, chemical, and mechanical properties of these particles. These elements significantly influence UNPs stability, surface reactivity, and interactions with the surrounding environment. Oxygen and carbon are essential in determining surface chemistry, while metals like Fe and Cr may affect magnetic properties, corrosion resistance, and overall reactivity. In addition to these primary elements, trace amounts of K, Sb, Cu, Ti, P, Mo, and Os were detected in fewer analyses. Although these elements were present in smaller quantities, they provided valuable insights into the unique properties of the NPs, such as their catalytic behaviour, conductivity, and potential immunotoxicity. Copper and titanium may play a role in catalytic reactions, whereas rarer elements such as Os and Mo may suggest specific industrial sources or environmental contamination. Since K, Os, and Mo were detected only in one analysis, their potential health effects were considered minimal. The concentration and presence of these elements have a significant impact on the behaviour of NPs in urban ecology. A Random Forest Regressor model predicted nanoparticle toxicity based on factors such as particle size, immunity exposure time, and exposure duration. Trained on synthetic data with noise to mimic biological variability, this model captured complex, nonlinear relationships using 30 decision trees. The results indicated that larger particles and longer exposure times were associated with higher toxicity, reflecting the multifaceted nature of nanoparticle risks. Elemental analysis of UNPs using EDX spectroscopy identified key elements (O, C, Ca, Si, Fe) that influence both the physical properties of nanoparticles and their biological effects, including oxidative stress and inflammation. The Decision Tree Regressor provided a more interpretable, threshold-based model, identifying specific cut-off points for toxicity levels. K-Means clustering grouped nanoparticles into low, medium, and high toxicity categories, helping to reveal how combinations of features influence toxicity. Together, these methods, along with elemental analysis, offer

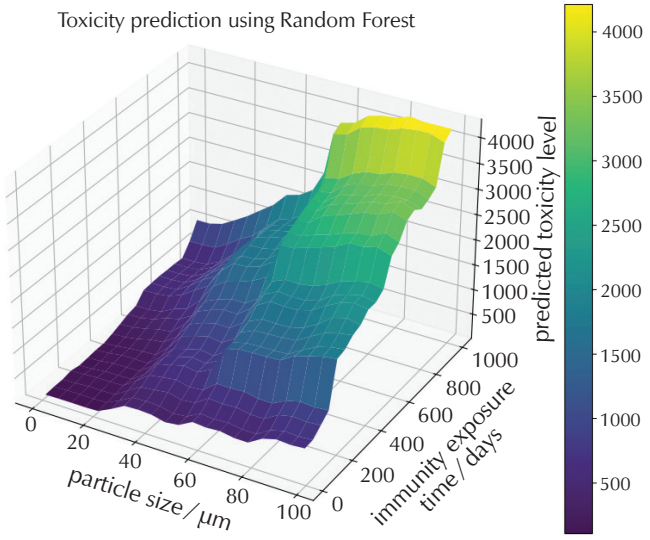


Fig. 4 – Surface plot displaying predicted toxicity levels as a function of particle size and immunity exposure time, with exposure days held constant at 15. The colour gradient represents toxicity intensity, illustrating that larger particle sizes and prolonged immunity exposure tend to result in higher toxicity predictions.

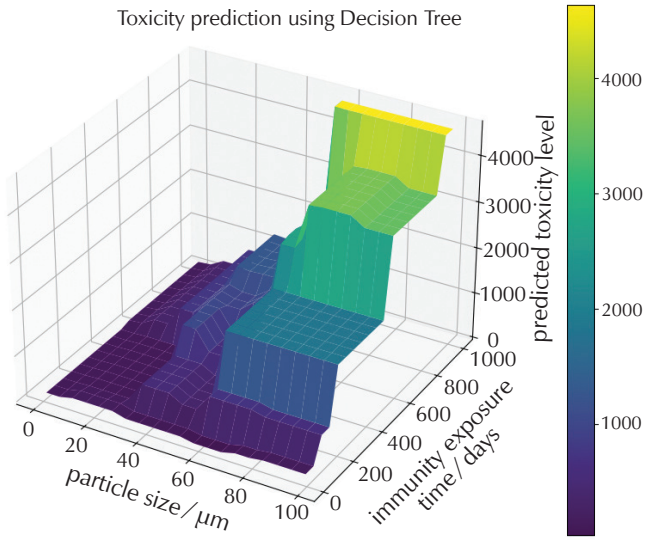


Fig. 5 – Predicted toxicity from a Decision Tree Regressor. The step-like structure of the surface illustrates the decision thresholds that divide the feature space, emphasising how specific particle size and immunity exposure intervals influence predicted toxicity.

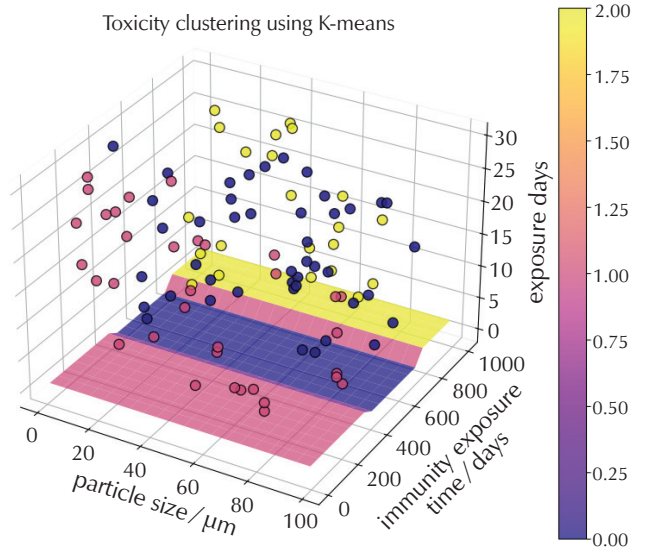


Fig. 6 – K-Means clustering results for nanoparticles representing particle size, immunity exposure time, and exposure days. Surface colours indicate cluster assignment, while scatter points represent individual nanoparticles, highlighting how features group according to predicted toxicity levels.

a robust framework for predicting toxicity, understanding nanoparticle behaviour, and supporting safety evaluations, particularly concerning long-term health risks from nanoparticle accumulation and immunological effects. Figs. 4–6 demonstrate the application of these models: Fig. 4 shows how toxicity varies with particle size and exposure time, while Fig. 5 illustrates toxicity thresholds from the Decision Tree, and Fig. 6 displays K-Means clustering results, categorising nanoparticles based on their toxicity levels.

Figs. 7–20 present advanced computational techniques for nanoparticle characterisation and risk profiling, demonstrating a range of advanced computational methods used to analyse nanoparticle properties, predict toxicity, bioaccumulation, and assess immune response. From TEM imaging to elemental analysis through EDX, as well as sophisticated machine-learning models and predictive simulations, these techniques offer a comprehensive approach to understanding nanoparticle behaviour and risk profiles. By integrating imaging data, elemental composition analysis, and machine-learning-driven predictions, these figures provided crucial insights into the dynamic and complex interactions of nanoparticles in biological and ecological systems.

The presented analyses compared predicted nanoparticle toxicity scores generated by machine-learning models with corresponding actual toxicity values, thereby serving as a validation of model performance. The model itself was informed by features derived from both TEM and EDX.

TEM contributed critical morphological descriptors such as particle size, shape, and aggregation state, which influence surface reactivity and biological interactions, while EDX provided quantitative elemental composition data. In particular, the model emphasised chromium (Cr) and copper (Cu) content as the primary determinants of toxicity, reflecting their known roles in promoting oxidative stress and associated cellular damage. By integrating these structural and compositional inputs, the machine-learning model effectively captured the underlying physicochemi-

cal factors governing nanoparticle toxicity, as evidenced by the strong agreement between predicted and actual values in the plot.

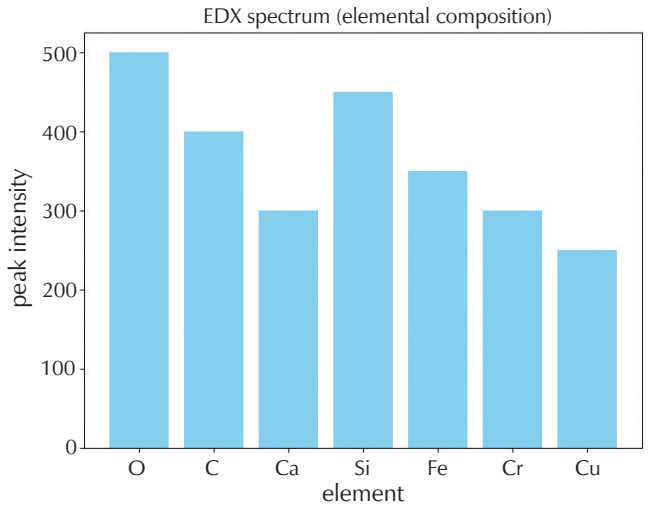


Fig. 7 – Computational modelling of an EDX spectrum plot, illustrating the elemental composition of a nanoparticle sample. The plot shows peak intensities for elements like O, C, Ca, and trace metals such as Fe and Cr, providing insights into the sample's chemical makeup. The intensity of these peaks is crucial for confirming the presence and abundance of specific elements, helping to assess the material's properties, including toxicity, bioaccumulation, and reactivity.

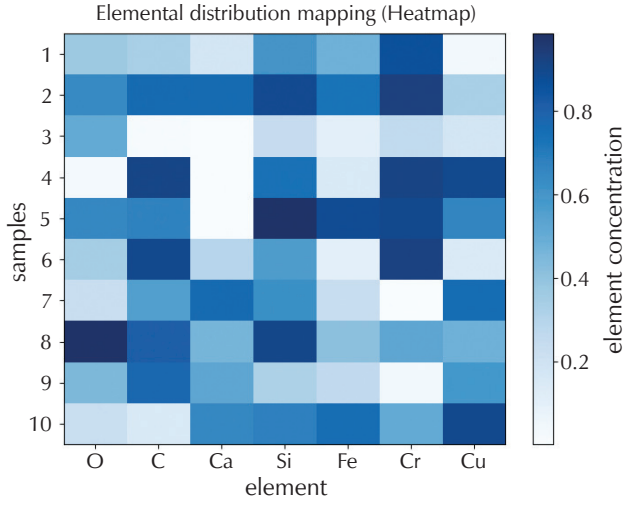


Fig. 8 – Elemental distribution heatmap visualises the spatial distribution and relative intensity of elements across the nanoparticle sample, with colour gradients indicating compositional heterogeneity, clustering, or localised enrichment. The EDX spectrum plot illustrates the elemental composition of the nanoparticle sample by showing peak intensities for O, C, Ca, Fe, and Cr, providing insight into chemical makeup and relative abundance.

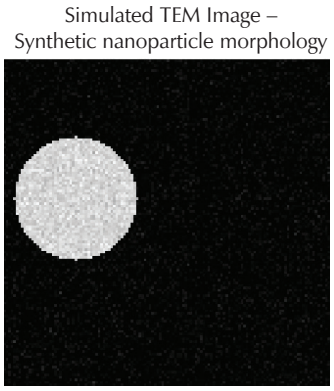


Fig. 9 – Single synthetic TEM-like image generated using computational methods that simulate the appearance of a nanoparticle under high-resolution TEM, showing a randomly sized and positioned circular particle with added noise to mimic realistic imaging conditions. This visualisation helps demonstrate how nanoparticles of different sizes and morphologies appear in TEM images. The synthetic image is particularly useful for testing feature extraction and machine-learning algorithms without requiring real experimental data. It provides insights into the particle's size, shape, and spatial distribution, which are essential for understanding nanoparticle characteristics.

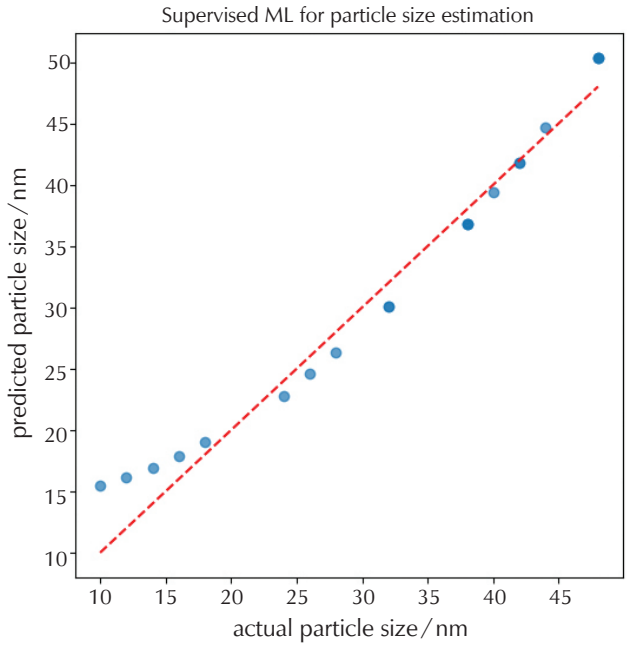


Fig. 10 – Comparison of the actual particle sizes with the predicted sizes obtained using a Linear Regression model trained on extracted features as surface area and aspect ratio. The corresponding Mean Absolute Error (MAE) quantifies the accuracy of the predictions, providing a numerical measure of model performance.

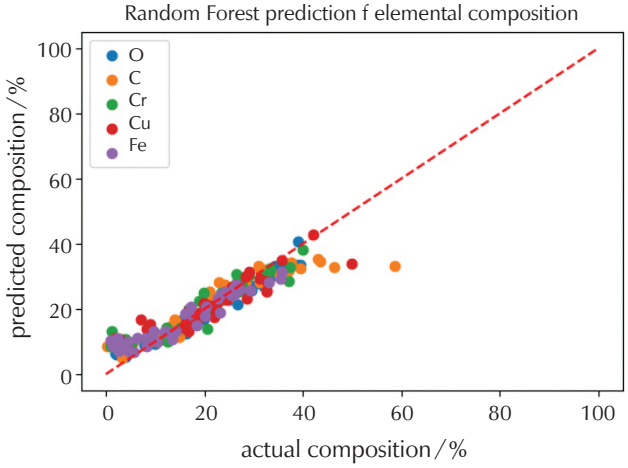


Fig. 11 – Comparison of the predicted elemental composition of nanoparticles from a Random Forest model with the actual simulated composition. Each element, O, C, Cr, Cu, Fe, is represented by a distinct set of points, and the diagonal red line indicates perfect prediction.

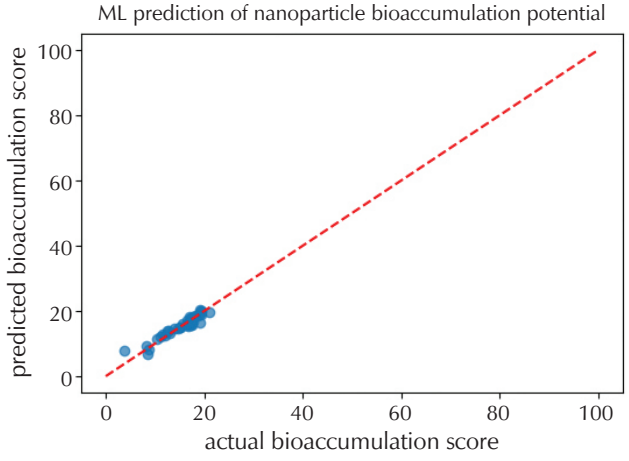


Fig. 13 – Comparison of the predicted nanoparticle bioaccumulation potential from a machine-learning model with the actual simulated values. The plot considers contributions from multiple metal elements, Cr, Cu, Fe, that influence bioaccumulation behaviour.

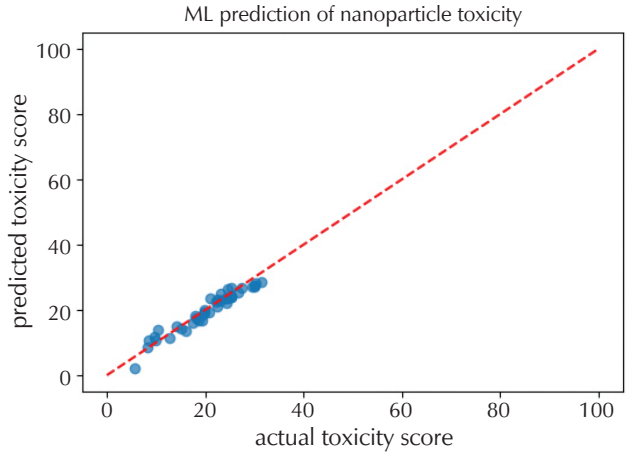


Fig. 12 – Comparison of the predicted nanoparticle toxicity scores from a machine-learning model with the actual simulated toxicity values. Toxicity is modelled as primarily dependent on Cr and Cu content, reflecting potential oxidative stress or harmful effects. The diagonal reference line indicates perfect agreement between predicted and actual toxicity scores.

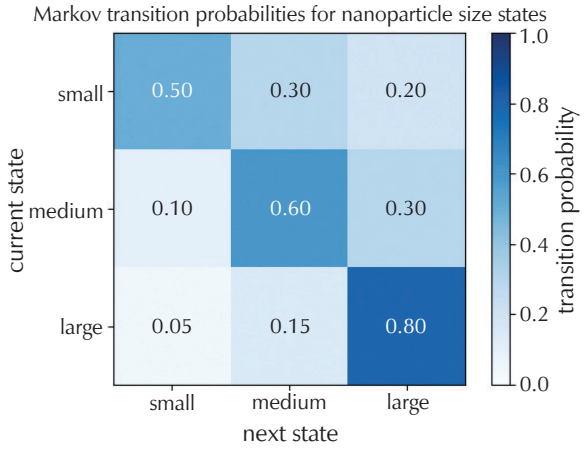


Fig. 14 – Markov transition probabilities for nanoparticle size states heatmap representing the Markov transition matrix for nanoparticle size states (Small, Medium, Large). Each cell shows the probability of a particle transitioning from its current size state to the next in one time step. The heatmap reveals that larger particles are more likely to stay large, while smaller particles have a higher probability of transitioning to medium or large states.

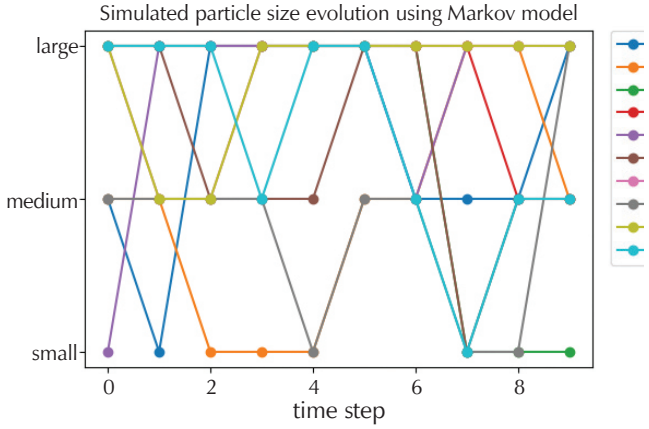


Fig. 15 – Simulated particle size evolution using Markov model time-series trajectories showing the size-state evolution of 10 representative nanoparticles over 10 discrete time steps simulated using the Markov model. Each line represents the trajectory of a particle's size state (small, medium, or large). The plot demonstrates stochastic transitions between size states, exhibiting the stability of larger particles, and more frequent transitions among small and medium particles. This visualisation provides insights into how nanoparticle populations evolve dynamically over time, helping to understand temporal changes in morphology and their potential effects on toxicity or bioaccumulation.

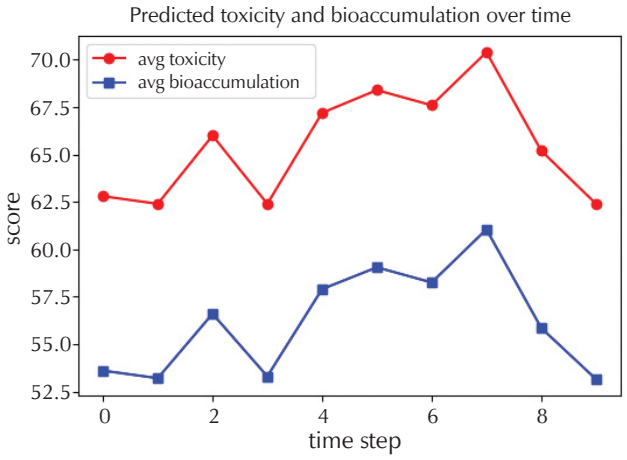


Fig. 16 – Predicted toxicity and bioaccumulation over time represents average toxicity and bioaccumulation scores across 10 time-steps for the nanoparticle population. Red circles represent average toxicity, while blue squares indicate average bioaccumulation potential. The plot shows how changes in particle size over time influence both toxicity and bioaccumulation, highlighting the relationship between nanoparticle characteristics and their biological interactions.

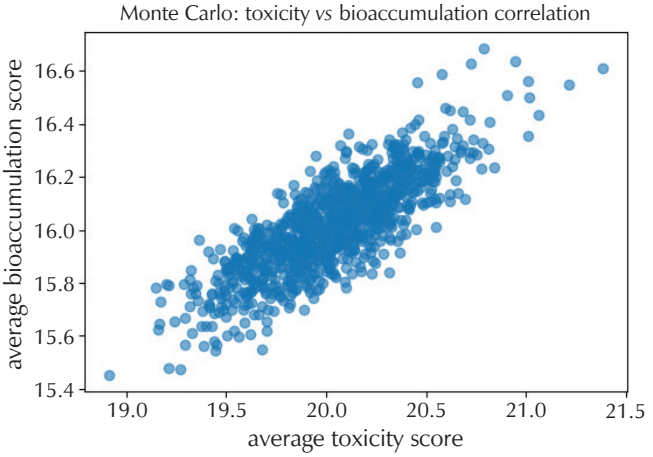


Fig. 17 – Monte Carlo simulation offers nanoparticle bioaccumulation potential histogram depicting predicted bioaccumulation scores, influenced by Cr, Cu, and Fe content in nanoparticles. This simulation demonstrates the variability in bioaccumulation risk within the simulated nanoparticle population, helping prioritise particles that may pose significant health risks, guiding safety evaluations and regulatory decisions.

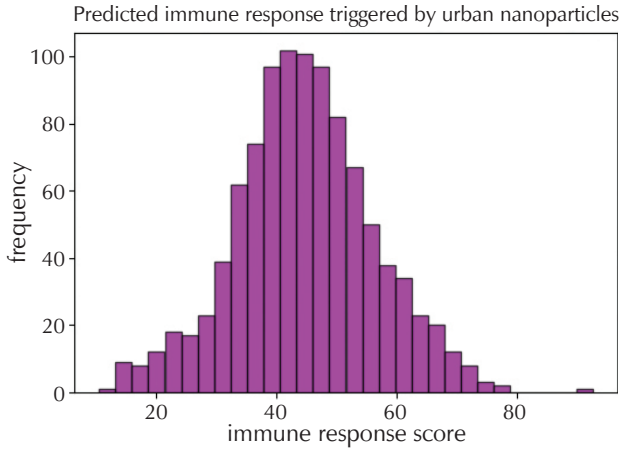


Fig. 18 – Predicted immune response triggered by urban nanoparticles histogram illustrates the distribution of immune response scores across all simulated nanoparticles. Immune response is modelled as a weighted combination of predicted toxicity and bioaccumulation, reflecting the increased likelihood of immune activation in particles with higher toxic potential or tissue accumulation. The plot highlights variability in immune responses and identifies high-risk nanoparticle populations requiring further safety evaluation.

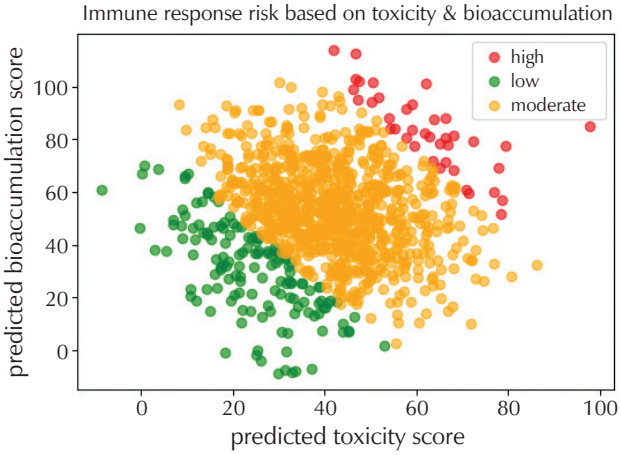


Fig. 19 – Immune response risk based on toxicity and bioaccumulation plot correlates predicted toxicity and bioaccumulation scores for each nanoparticle and categorises immune response risk as low, moderate, or high. Nanoparticles exhibiting both high toxicity and bioaccumulation fall within the high-risk category, indicating an increased potential for immuno-toxic effects. This presentation aids in identifying nanoparticle characteristics most strongly associated with immune activation.

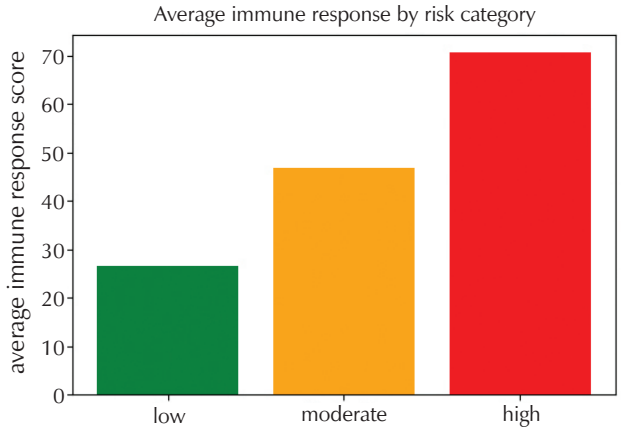


Fig. 20 – Average immune response by risk category chart summarises the average immune response scores for low, moderate and high-risk nanoparticle groups. The data clearly shows that high-risk nanoparticles trigger the strongest immune activation, with significantly higher response scores compared to low-risk particles, which exhibit minimal immune response.

4 Discussion

The structural and elemental characterisation of urban nanoparticles (UNPs) provided important insight into their environmental behaviour and potential biological effects. As demonstrated in Fig. 1, transmission electron microscopy (TEM) revealed a highly heterogeneous nanoparticle population ranging from 50 to 500 nm, with a substantial fraction below 100 nm. This ultrafine fraction is particularly significant due to its enhanced ability to penetrate deep into the respiratory tract and potentially enter systemic circulation. The observed irregular, angular, and agglomerated morphologies indicate that these particles originated from multiple urban sources, including combustion processes, industrial emissions, and resuspended post-earthquake debris.

The compositional complexity of UNPs is further highlighted in Figs. 2 and 3. Energy-dispersive X-ray spectroscopy (EDX) analysis identified dominant elements such as O, C, Ca, and Si, alongside transition metals, including Fe, Cr, and Cu, as well as trace elements (*e.g.*, Sb, Mo, Os, Ti, and P). These elements play a critical role in determining nanoparticle surface chemistry, reactivity, and toxicological behaviour. In particular, transition metals such as Cr and Cu, are strongly associated with reactive oxygen species (ROS) generation, leading to oxidative stress, inflammation, and cellular damage. Even trace elements, although present in low concentrations, may contribute to cumulative toxicity under long-term exposure conditions. The variability observed across these figures reflects the multifactorial nature of urban particulate pollution, especially in post-disaster environments.

The relationship between nanoparticle properties and toxicity was explored through computational modelling in Figs. 4–6. The surface plot (Fig. 4) demonstrates that toxicity increased with both particle size and exposure duration. The Decision Tree model (Fig. 5) provided interpretable thresholds that define toxicity levels, while K-means clustering (Fig. 6) categorised nanoparticles into low-, moderate-, and high-toxicity groups. These findings confirm that toxicity arises from the interaction of multiple physicochemical parameters rather than a single factor.

Further integration of structural and compositional data is presented in Figs. 7–12. The EDX spectrum (Fig. 7) and elemental distribution heatmap (Fig. 8) confirm the presence and relative abundance of key elements, while the synthetic TEM image (Fig. 9) supports feature extraction for modelling applications. Predictive model performance is demonstrated in Fig. 10 (particle size prediction), Fig. 11 (elemental composition), and Fig. 12 (toxicity), all showing strong agreement between predicted and actual values. Notably, Fig. 12 identifies chromium (Cr) and copper (Cu) as dominant contributors to toxicity, consistent with their known roles in oxidative stress and inflammatory responses.

Temporal dynamics of nanoparticle behaviour are illustrated in Figs. 13–16. Bioaccumulation predictions (Fig. 13) indicate the influence of metal composition on accumulation potential. Markov transition analysis (Fig. 14) shows that larger particles tended to remain stable, whereas smaller particles exhibited more frequent transitions between size states. These dynamics were further visualised in the time-series trajectories (Fig. 15), demonstrating the stochastic evolution of nanoparticle populations. The combined impact on biological outcomes is shown in Fig. 16, where both toxicity and bioaccumulation varied over time, confirming that nanoparticle-associated risks are dynamic rather than static.

Uncertainty and variability in nanoparticle behaviour were addressed using Monte Carlo simulation in Fig. 17, which reveals a broad distribution of bioaccumulation potential across the particle population. This variability is critical for identifying high-risk subsets of nanoparticles. The immunological implications were further explored in Figs. 18–

20. The immune response distribution (Fig. 18) highlights variability in biological responses, while Fig. 19 classifies nanoparticles into low-, moderate-, and high-risk categories based on combined toxicity and bioaccumulation parameters. Fig. 20 confirms that high-risk nanoparticles induced significantly stronger immune responses, reinforcing the link between physicochemical properties and immuno-toxic effects.

Overall, the integration of TEM imaging (Fig. 1), EDX compositional analysis (Figs. 2–3), and advanced computational modelling (Figs. 4–20) provided a comprehensive framework for understanding nanoparticle behaviour and associated risks. The strong predictive performance of the models demonstrated that particle size and metal composition were key determinants of toxicity and immune response. However, it is important to note that the modelling approaches were based on simulated data and may not have fully captured the complexity of real biological systems. Future research should focus on experimental validation and the inclusion of additional parameters such as surface charge, particle coating, and environmental interactions.

Table 1 compares the toxicological effects of the various NPs, drawn from *in vivo* or *in vitro* experimentation stud-

Table 1 – Outline of the conducted *in vivo* or *in vitro* experimentation models with various NPs

NPs	*In vivo* or *in vitro* models	Dose level	NP size	Effects – Ref.
CBNPs	Mice	95 μg kg^{-1}	14 nm	Inflammation, accumulation[46]
CNPs	Macrophage, mouse	–	–	Apoptosis, accumulations[88]
Si	Mice	0.25 mg kg^{-1}	50 nm	Genotoxic, cytotoxic, transcriptomic responses[59]
SiO_2	Cells	–	~ 30 nm	Metastasis[52]
Si	Mice	–	~ 45 nm	Biodistribution and organ deposition[55]
Si	Mouse	12.5–100 μg ml^{-1}	10–15 nm	Inflammation, DNA damage, toxicity, oxidative stress[60]
Si- TiO_2	Mice	–	70, 35 nm	Pregnancy complications[79]
Si	Human keratinocytes (HaCaT)	0–100 μg ml^{-1}	15–100 nm	Reactive oxygen species (ROS), DNA damage, cytotoxicity[87]
TiO_2	Hepatocytes	5–200 mg kg^{-1}	5–90 nm	Nerve cell damage[81]
TiO_2	Mice	5 g kg^{-1}	25–155 nm	Liver damage[82]
Asbestos	Mice	–	< 1 μm, > 20 μm	Bronchiolar epithelial damage[85]
CeO_2, SnO_2, Fe_2O_3	Microbial biomass	0–100 mg kg^{-1}	< 2–53 μm	Toxicity[26]
Fe_2O_3	Mouse fibroblast cells	–	20–30 nm	Cytotoxicity[92]
DIONPs	Lymphocytes	0.008–1 mg ml	20–30 nm	Immune response (IR), immuno-toxicity[91]
CuO	Mice	0.8, 2.11 l min^{-1}	3–11 nm	Immune response (IR)[97]
CuO	Lung epithelial cells	–	50 nm	Genotoxicity[65]
CuO, SiO_2, Fe_2O_3	Airway epithelial cells	4–400 μg cm^{-2}	30 nm	Cytotoxicity[66]
Al_2O_3	Rats	2000 mg kg^{-1}	30–40 nm	Genotoxicity[69]
Cr	*Saccobranchus fossilis*	0.1–3.2 mg l^{-1} for 28 days	–	Immune response (IR)[70]
Cr	Mud crabs	1.4–312.2 mg kg^{-1}	–	Accumulation, cancer[71]
Cr	Apoptotic cell, mice	–	–	Oxygen species (ROS)[72]
SO_2	Rats	2200 ppm for 10 min	–	Inflammation, fibrotic respiratory disease[75]
SO_2	Asthmatic rats	–	–	Inflammatory, immune responses (IR), asthma[48]
MgO	Human liver organoid models, rat convulsion model	–	–	Hepatotoxic effects[73]
MgO	*Phytophthora infestans*	50 μg ml^{-1}	–	Toxicity[74]
Asbestos	–	–	–	immune responses[86]
Fe_2O_3, Fe_3O_4, Sb_2O_3, Au, TiO_2, Co, Ag	Erythroid progenitors	5 μg ml^{-1}	–	Toxicity[93]
MoO_3	Golden Syrian hamsters	5 mg m^{-3}, 4 h/8 days	–	Lung damage, cell death[94]
MoO_3	*Candida albicans, Aspergillus niger*	–	75 nm	Antifungal activity[95]
AlO_2	*Rats*	6–25 mg kg^{-1}	75 nm	Genotoxicity[96]

ies. The analysis indicates that different NPs had varying toxicological profiles, ranging from cytotoxicity and genotoxicity to immune responses and inflammation. For example, copper oxide (CuO) NPs cause immune responses, potentially leading to chronic inflammation and autoimmune disorders, while also inducing genotoxicity in lung cells, suggesting a carcinogenic potential. Similarly, SiO_2, TiO_2, and Fe_2O_3 NPs show respiratory toxicity, raising concerns for respiratory health in industrial and urban areas. Exposure to chromium (Cr^{6+}) and sulphur dioxide (SO_2) further emphasises their role in inflammation and respiratory diseases.

Si-based NPs, for instance, are associated with severe effects like genotoxicity, cytotoxicity, inflammation, and oxidative stress. These NPs, particularly in the size range of 30–45 nm, accumulate in organs and contribute to systemic toxicity. Carbon-based NPs, while less potent, are linked to respiratory irritation, inflammation, and cell death. Similarly, Cr-based NPs generate reactive oxygen species (ROS), leading to oxidative stress and cancer, while Cu-based NPs contribute to inflammation, genotoxicity, and tissue damage. SO_2 exposure, although not traditionally classified as an NP, contributes to asthma and chronic respiratory issues, underlining the significance of pollutants in urban areas.

The overall immuno-toxicological effects of the NPs studied here vary according to their elemental composition and molecular forms. As evidenced by the previous studies, particles such as Si, Cu, Cr, and C have profound impacts on immune responses, inflammation, and organ-specific toxicity. The interactions between these NPs and biological systems depend on particle size, surface properties, and chemical composition. The results highlight the complexity of these interactions and the need for further research to fully understand their long-term health risks.

The diverse elemental composition and structural properties of UNPs play a significant role in their toxicological profiles. This study emphasises the importance of assessing not only the physical properties of these particles but also their chemical composition and interactions with biological systems. The findings support the need for more comprehensive risk assessments for mitigation strategies, particularly in urban areas with high pollution levels, to better understand the health implications of chronic exposure to such particles. Despite the limitations, the findings in this experimental and computational study offer significant insight into the mechanisms driving nanoparticle toxicity, and highlight the importance of multidisciplinary approaches for improving risk assessment of urban particulate matter, particularly in post-earthquake environments.

5 Conclusion

This experimental and computational study provides a comprehensive assessment of urban nanoparticles (UNPs) generated in a post-earthquake environment, highlighting their structural complexity, diverse elemental composition, and potential implications for human health. TEM analysis revealed a highly heterogeneous particle population, including a significant proportion of ultrafine particles capable of deep respiratory penetration. EDX spectroscopy confirmed the presence of both major elements (O, C, Ca, Si) and transition metals such as Fe, Cr, and Cu, which are known to influence nanoparticle reactivity and toxicity. Computational modelling approaches demonstrated that nanoparticle toxicity is not governed by a single parameter but rather by the interaction of particle size, composition, and exposure duration. Machine-learning models identified chromium and copper as key contributors to oxidative stress, while stochastic simulations highlighted the dynamic nature of nanoparticle behaviour, including bioaccumulation potential and temporal variability. These findings emphasise that nanoparticle-associated risks evolve over time and depend on complex environmental and biological interactions. Comparative evaluation with *in vivo* or *in vitro* experimentation model studies suggests that the identified nanoparticles may induce oxidative stress, inflammation, and immune dysregulation, particularly due to their metal-rich composition and ultrafine size fraction. Although the modelling framework provides valuable predictive insight, the absence of experimental biological validation remains a limitation. This work underscores the importance of integrating advanced imaging, compositional analysis, and computational modelling to better understand the health risks associated with urban particulate matter, particularly in post-disaster settings.

References
Literatura

1. *C. A. Pope, D. W. Dockery*, Health effects of fine particulate air pollution: Lines that connect, J. Air Waste Manage. Assoc. **56** (2006) 709–742, doi: https://doi.org/10.1080/10473289.2006.10464485.
2. *R. Chen, C. Chen*, Environment, Health and Safety Issues in Nanotechnology, in: B. Bhushan (Ed.), Springer Handbook of Nanotechnology, Springer, Berlin, Heidelberg (2017), doi: https://doi.org/10.1007/978-3-662-54357-3_45.
3. *V. H. Liao*, Nanoparticles in the environment and nanotoxicology, Nanomaterials **13** (2023) 1053, doi: https://doi.org/10.3390/nano13061053.
4. *D. Srivastava, N. Sharma, V. Arya, B. Arya, A. Kumar, R. Amarowicz*, Nanotoxicology: A threat to the environment and human health, in: A. Balkrishna, N. Thakur, V. Arya, A. Kumar (Eds.), Nanotechnology, Springer, Singapore, 2024, doi: https://doi.org/10.1007/978-981-97-6814-1_8.
5. *V. Cukic, V. Lovre, D. Dragisic, A. Ustamujic*, Asthma and chronic obstructive pulmonary disease (COPD) – Differences and similarities, Mater. Soc. Med. **24** (2012) 100–105, doi: https://doi.org/10.5455/msm.2012.24.100-105.
6. *R. Kumar, A. Kumar, S. Bhardwaj, M. Sikarwar, S. Sriwastaw, G. Sharma, M. Gupta*, Nanotoxicity unveiled: Evaluating exposure risks and assessing the impact of nanoparticles on human health, J. Trace Elem. Miner. **13** (2025) 100252, doi: https://doi.org/10.1016/j.jtemin.2025.100252.
7. *M. Sajid, M. Ilyas, C. Basheer, M. Tariq, M. Daud, N. Baig, F. Shehzad*, Impact of nanoparticles on human and environment: review of toxicity factors, exposures, control strategies, and future prospects, Environ. Sci. Pollut. Res. **22** (2015) 4122–4143, doi: https://doi.org/10.1007/s11356-014-3994-1.
8. *G. Martínez, M. Merinero, M. Pérez-Aranda, E.M. Pérez-So-*

riano, T. Ortiz, B. Begines, A. Alcudia, Environmental Impact of Nanoparticles' Application as an Emerging Technology: A Review, Materials **14** (2020) 166, doi: https://doi.org/10.3390/ma14010166.

9. *S. M. Alizadeh, J. F. Qarachal, E. Sheidaee*, Understanding the ecological impacts of nanoparticles: Risks, monitoring, and mitigation strategies, Nanotechnol. Environ. Eng. **10** (2025) 6, doi: https://doi.org/10.1007/s41204-024-00403-7.
10. *W. Qamar, S. Gulia, M. Athar, R. Ahmad, M. T. Imam, P. Chandra, B. P. Singh, R. Haque, M. I. Hassan, S. Rahman*, An insight into impact of nanomaterials toxicity on human health, PeerJ **12** (2024) e17807, doi: https://doi.org/10.7717/peerj.17807.
11. *M. A. Saifi, W. Khan, C. Godugu*, Cytotoxicity of nanomaterials: Using nanotoxicology to address the safety concerns of nanoparticles, Pharm. Nanotechnol. **6** (2018) 3–16, doi: https://doi.org/10.2174/2211738505666171023152928.
12. *E. Asmatulu, M. N. Andalib, B. Subeshan, F. Abedin*, Impact of nanomaterials on human health: A review, Environ. Chem. Lett. **20** (2022) 2509–2529, doi: https://doi.org/10.1007/s10311-022-01430-z.
13. *P. T. King*, Inflammation in chronic obstructive pulmonary disease and its role in cardiovascular disease and lung cancer, Clin. Transl. Med. **4** (2015) 68, doi: https://doi.org/10.1186/s40169-015-0068-z.
14. *Y. A. Alemayehu, S. L. Asfaw, T. A. Terfie*, Exposure to urban particulate matter and its association with human health risks, Environ. Sci. Pollut. Res. **27** (2020) 27491–27506, doi: https://doi.org/10.1007/s11356-020-09132-1.
15. *M. M. Glovsky, A. G. Miguel, G. R. Cass*, Particulate air pollution: possible relevance in asthma, Allergy Asthma Proc. **18** (1997) 163–166, doi: https://doi.org/10.2500/108854197778984392.
16. *W. Kreyling, S. Hirn, C. Schleh*, Nanoparticles in the lung, Nat. Biotechnol. **28** (2010) 1275–1276, doi: https://doi.org/10.1038/nbt.1735.
17. *B. A. Jamuna, V. Ravishankar*, Environmental risk, human health, and toxic effects of nanoparticles, in: B. I. Kharisov, O. V. Kharissova, H.V.R. Dias (Eds.), Nanomaterials for Environmental Protection, Wiley, **31**, 2014, doi: https://doi.org/10.1002/9781118845530.ch31.
18. *S. Omari Shekaftik, N. Mehrparvar, Z. Peivandi, S. T. Banasaz, A. Rafieepour, N. Moghadasi, A. Ashtarinezhad*, Occupational exposure to nanomaterials: A scoping review, J. Clust. Sci. **36** (2025) 152, doi: https://doi.org/10.1007/s10876-025-02864-5.
19. *E. A. Kumah, R. D. Fopa, S. Harati, P. Boadu, F. V. Zohoori, T. Pak*, Human and environmental impacts of nanoparticles: A scoping review of the current literature, BMC Public Health **23** (2023) 1059, doi: https://doi.org/10.1186/s12889-023-15958-4.
20. *G. Oberdörster, A. Maynard, K. Donaldson, V. Castranova, J. Fitzpatrick, K. Ausman, J. Carter, B. Karn, W. Kreyling, D. Lai, S. Olin, N. Monteiro-Riviere, D. Warheit, H. Yang & A report from the ILSI Research Foundation/Risk Science Institute Nanomaterial Toxicity Screening Working Group*, Principles for characterizing the potential human health effects from exposure to nanomaterials: Elements of a screening strategy, Part. Fibre Toxicol. **2** (2005) 8, doi: https://doi.org/10.1186/1743-8977-2-8.
21. *A. L. Moreno-Ríos, L. P. Tejeda-Benítez, C. F. Bustillo-Lecompte*, Sources, characteristics, toxicity, and control of ultrafine particles: An overview, Geosci. Front. **13** (2022) 101147, doi: https://doi.org/10.1016/j.gsf.2021.101147.
22. *V. Ramchandran, J. M. Gernand*, Examining the *in vivo* pulmonary toxicity of engineered metal oxide nanomaterials using a genetic algorithm-based dose-response-recovery clustering model, Comput. Toxicol. **13** (2020) 100113, doi: https://doi.org/10.1016/j.comtox.2019.100113.
23. *A. Elsaesser, C. V. Howard*, Toxicology of nanoparticles, Adv. Drug Deliv. Rev. **64** (2012) 129–137, doi: https://doi.org/10.1016/j.addr.2011.09.001.
24. *K. Donaldson, D. Brown, A. Clouter, R. Duffin, W. MacNee, L. Renwick, L. Tran, V. Stone*, The pulmonary toxicology of ultrafine particles, J. Aerosol Med. **15** (2002) 213–220, doi: https://doi.org/10.1089/089426802320282338.
25. *A. A. Aljabali, M. A. Obeid, R. M. Bashatwah, Á. Serrano-Aroca, V. Mishra, Y. Mishra, M. El-Tanani, A. Hromić-Jahjefendić, D. N. Kapoor, R. Goyal, G. A. Naikoo, M. M. Tambuwala*, Nanomaterials and their impact on the immune system, Int. J. Mol. Sci. **24** (2023) 2008, doi: https://doi.org/10.3390/ijms24032008.
26. *L. Vittori Antisari, S. Carbone, A. Gatti, G. Vianello, P. Nannipieri*, Toxicity of metal oxide (CeO_2, Fe_3O_4, SnO_2) engineered nanoparticles on soil microbial biomass and their distribution in soil, Soil Biol. Biochem. **60** (2013) 87–94, doi: https://doi.org/10.1016/j.soilbio.2013.01.016.
27. *E. R. Bordin, W. A. Ramsdorf, L. M. L. Domingos, L. P. S. Miranda, N. P. Mattoso Filho, M. M. Cestari*, Ecotoxicological effects of zinc oxide nanoparticles (ZnO-NPs) on aquatic organisms: Current research and emerging trends, J. Environ. Manag. **349** (2024) 119396, doi: https://doi.org/10.1016/j.jenvman.2023.119396.
28. *R. Podila, J. M. Brown*, Toxicity of engineered nanomaterials: a physicochemical perspective, J. Biochem. Mol. Toxicol. **27** (2013) 50–55, doi: https://doi.org/10.1002/jbt.21442.
29. *A. Gupta, S. Kumar, V. Kumar*, Challenges for Assessing Toxicity of Nanomaterials, in: Biochemical Toxicology – Heavy Metals and Nanomaterials, IntechOpen, 2020, doi: https://doi.org/10.5772/intechopen.89601.
30. *D. Hristozov, I. Malsch*, Hazards and Risks of Engineered Nanoparticles for the Environment and Human Health, Sustainability **1** (2009) 1161–1194, doi: https://doi.org/10.3390/su1041161.
31. *S. Hofer, N. Hofstätter, B. Punz, I. Hasenkopf, L. Johnson, M. Himly*, Immunotoxicity of nanomaterials in health and disease: Current challenges and emerging approaches for identifying immune modifiers in susceptible populations, WIREs: Nanomed. Nanobiotechnol. **14** (6) (2022) e1804, doi: https://doi.org/10.1002/wnan.1804.
32. *J. W. Card, D. C. Zeldin, J. C. Bonner, E. R. Nestmann*, Pulmonary applications and toxicity of engineered nanoparticles, Am. J. Physiol. Lung Cell Mol. Physiol. **295** (2008) L400–L411, doi: https://doi.org/10.1152/ajplung.00041.2008.
33. *X. Q. Liu, R. Z. Tang*, Biological responses to nanomaterials: understanding nano-bio effects on cell behaviors, Drug Deliv. **24** (2017) 1–15, doi: https://doi.org/10.1080/10717544.2017.1375577.
34. *Y. Liu, J. Hardie, X. Zhang, V. M. Rotello*, Effects of engineered nanoparticles on the innate immune system, Semin. Immunol. **34** (2017) 25–32, doi: https://doi.org/10.1016/j.smim.2017.09.011.
35. *W. N. Missaoui, R. D. Arnold, B. S. Cummings*, Toxicological status of nanoparticles: What we know and what we don't know, Chem. Biol. Interact. **295** (2018) 1–12, doi: https://doi.org/10.1016/j.cbi.2018.07.015.
36. *J. Y. Liu, C. M. Sayes*, A toxicological profile of silica nanoparticles, Toxicol. Res. **11** (2022) 565–582, doi: https://doi.org/10.1093/toxres/tfac038.
37. *A. Nel, T. Xia, L. Mädler, N. Li*, Toxic potential of materials at the nanolevel, Science **311** (2006) 622–627, doi: https://

doi.org/10.1126/science.1114397.

38. *S. Sonwani, S. Madaan, J. Arora, S. Suryanarayan, D. Rangra, N. Mongia, N. Mongia, T. Vats, P. Saxena*, Inhalation exposure to atmospheric nanoparticles and its associated impacts on human health: A review, Front. Sustain. Cities **3** (2021) 690444, doi: https://doi.org/10.3389/frsc.2021.690444.
39. *M. Summer, R. Ashraf, S. Ali, H. Bach, S. Noor, Q. Noor, S. Riaz, R. R. M. Khan*, Inflammatory response of nanoparticles: Mechanisms, consequences, and strategies for mitigation, Chemosphere **363** (2024) 142826, doi: https://doi.org/10.1016/j.chemosphere.2024.142826.
40. *K. Pondman, S. Le Gac, U. Kishore*, Nanoparticle-induced immune response: Health risk versus treatment opportunity? Immunobiology **228** (2023) 152317, doi: https://doi.org/10.1016/j.imbio.2022.152317.
41. *S. Sabir, A. Jan*, Physiology, Immune Response, StatPearls (2026), StatPearls Publishing, Treasure Island (FL).
42. *W. Warisnoicharoen, P. Hongpiticharoen, S. Lawanprasert*, Alteration in enzymatic function of human cytochrome P450 by silver nanoparticles, Res. J. Environ. Toxicol. **5** (2011) 58–64, doi: https://doi.org/10.3923/rjet.2011.58.64.
43. *P. P. Fu, Q. Xia, H. M. Hwang, P. C. Ray, H. Yu*, Mechanisms of nanotoxicity: Generation of reactive oxygen species, J. Food Drug Anal. **22** (2014) 64–75, doi: https://doi.org/10.1016/j.jfda.2014.01.005.
44. *P. D. Dwivedi, A. Tripathi, K. M. Ansari, R. Shanker, M. Das*, Impact of nanoparticles on the immune system, J. Biomed. Nanotechnol. **7** (2011) 193–194, doi: https://doi.org/10.1166/jbn.2011.1264.
45. *A. Kunzmann, B. Andersson, T. Thurnherr, H. Krug, A. Scheynius, B. Fadeel*, Toxicology of engineered nanomaterials: Focus on biocompatibility, biodistribution and biodegradation, Biochim. Biophys. Acta **1810** (2011) 361–373, doi: https://doi.org/10.1016/j.bbagen.2010.04.007.
46. *Y. Niwa, Y. Hiura, H. Sawamura, N. Iwai*, Inhalation exposure to carbon black induces inflammatory response in rats, Circ. J. **72** (2008) 144–149, doi: https://doi.org/10.1253/circj.72.144.
47. *M. A. Vlasova, J. Rytkönen, J. Riikonen, O. S. Tarasova, J. Mönkäre, M. Kovalainen, A. Närvänen, J. Salonen, K.-H. Herzig, V.-P. Lehto, K. Järvinen*, Nanocarriers and the delivered drug: Effect interference due to intravenous administration, Eur. J. Pharm. Sci. **63** (2014) 96–102, doi: https://doi.org/10.1016/j.ejps.2014.06.011.
48. *R. Li, X. Kou, J. Tian, Z. Meng, Z. Cai, F. Cheng, C. Dong*, Effect of sulfur dioxide on inflammatory and immune regulation in asthmatic rats, Chemosphere **112** (2014) 296–304, doi: https://doi.org/10.1016/j.chemosphere.2014.04.065.
49. *Z. Haidar, K. Fatema, S. S. Shoily, A. A. Sajib*, Disease-associated metabolic pathways affected by heavy metals and metalloids, Toxicol. Rep. **10** (2023) 554–570, doi: https://doi.org/10.1016/j.toxrep.2023.04.010.
50. *P. Marrack, A. S. McKee, M. W. Munks*, Towards an understanding of the adjuvant action of aluminum, Nat. Rev. Immunol. **9** (2009) 287–293, doi: https://doi.org/10.1038/nri2510.
51. *B. De Berardis, E. Incocciati, S. Massera, G. Gargaro, L. Paoletti*, Airborne silica levels in an urban area, Sci. Total Environ. **382** (2007) 251–258, doi: https://doi.org/10.1016/j.scitotenv.2007.04.044.
52. *H. Dai, Q. Fan, Z. Fei, Q. Ma, Q. Yang, J. Chu, X. Zhou, Y. Zhang, Z. Dong, F. Xu, B. Wang, R. Sun, Y. Shen, R. Xie, R. Li, C. Wang*, Systemically administered silica nanoparticles result in diminished T-cell response in lung, Nano Today **42** (2022) 101332, doi: https://doi.org/10.1016/j.nantod.2021.101332.
53. *W. Seaton, K. MacNee, D. Donaldson, D. Godden*, Particulate air pollution and acute health effects, Lancet **345** (1995) 176–178, doi: https://doi.org/10.1016/S0140-6736(95)90173-6.
54. *L. H. Ao, Y. G. Wei, H. R. Tian, H. Zhao, J. Li, J. Q. Ban*, Advances in the study of silica nanoparticles in lung diseases, Sci. Total Environ. **912** (2024) 169352, doi: https://doi.org/10.1016/j.scitotenv.2023.169352.
55. *X. He, H. Nie, K. Wang, W. Tan, X. Wu, P. Zhang*, *In vivo* study of biodistribution and urinary excretion of surface-modified silica nanoparticles, Anal. Chem. **80** (2008) 9597–9603, doi: https://doi.org/10.1021/ac801882g.
56. *H. Nabeshi, T. Yoshikawa, K. Matsuyama, Y. Nakazato, S. Tochigi, S. Kondoh, T. Hirai, T. Akase, K. Nagano, Y. Abe, Y. Yoshioka, H. Kamada, N. Itoh, S.-i. Tsunoda, Y. Tsutsumi*, Amorphous nanosilica induces endocytosis-dependent ROS generation and DNA damage in human keratinocytes, Part. Fibre Toxicol. **8** (2011) 1, doi: https://doi.org/10.1186/1743-8977-8-1.
57. *S. Murugadoss, D. Lison, L. Godderis, S. Van Den Brule, J. Mast, F. Brassinne, N. Sebaihi, P. H. Hoet*, Toxicology of silica nanoparticles: An update, Arch. Toxicol. **91** (2017) 2967–3010, doi: https://doi.org/10.1007/s00204-017-1993-y.
58. *L. Chen, J. Liu, Y. Zhang, G. Zhang, Y. Kang, A. Chen, X. Feng, L. Shao*, The toxicity of silica nanoparticles to the immune system, Nanomedicine **13** (2018) 1939–1962, doi: https://doi.org/10.2217/nnm-2018-0076.
59. *A. Nemmar, P. Yuvaraju, S. Beegam, J. Pathan, E. E. Kazzam, B. H. Ali*, Oxidative stress, inflammation, and DNA damage in multiple organs of mice acutely exposed to amorphous silica nanoparticles, Int. J. Nanomed. **11** (2016) 919–928, doi: https://doi.org/10.2147/IJN.S92278.
60. *N. Decan, D. Wu, A. Williams, S. Bernatchez, M. Johnston, M. Hill, S. Halappanavar*, Characterization of *in vitro* genotoxic, cytotoxic, and transcriptomic responses following exposures to amorphous silica of different sizes, Mutat. Res. Genet. Toxicol. Environ. Mutagen. **796** (2016) 8–22, doi: https://doi.org/10.1016/j.mrgentox.2015.11.011.
61. *C. Liang, Q. Xiang, W. M. Cui, J. Fang, N. N. Sun, X. P. Zhang, Y. N. Li, H. Yang, Z. Yu, X. D. Jia*, Subchronic oral toxicity of silica nanoparticles and silica microparticles in rats, Biomed. Environ. Sci. **31** (2018) 197–207, doi: https://doi.org/10.3967/bes2018.025.
62. *M. d'Amora, F. Liendo, F. A. Deorsola, S. Bensaid, S. Giordani*, Toxicological profile of calcium carbonate nanoparticles for industrial applications, Colloids Surf. B: Biointerfaces **190** (2020) 110947, doi: https://doi.org/10.1016/j.colsurfb.2020.110947.
63. *J. Tulinska, M. L. Mikusova, A. Liskova, M. Busova, V. Masanova, I. Uhnakova, E. Rollerova, R. Alacova, Z. Krivosikova, L. Wsolova, M. Dusinska, M. Horvathova, M. Szabova, N. Lukan, M. Stuchlikova, D. Kuba, Z. Vecera, P. Coufalik, K. Krumal, L. Alexa, L. Vrlikova, M. Buchtova, J. Dumkova, P. Piler, V. Thon, P. Mikuska*, Copper Oxide Nanoparticles Stimulate the Immune Response and Decrease Antioxidant Defense in Mice After Six-Week Inhalation, Front. Immunol. **13** (2022) 874253, doi: https://doi.org/10.3389/fimmu.2022.874253.
64. *R. K. Shukla, A. Badiye, K. Vajpayee, N. Kapoor*, Genotoxic Potential of Nanoparticles: Structural and Functional Modifications in DNA, Front. Genet. **12** (2021) 728250, doi: https://doi.org/10.3389/fgene.2021.728250.
65. *M. Ahamed, M. A. Siddiqui, M. J. Akhtar, I. Ahmad, A. B. Pant, H. A. Alhadlaq*, Genotoxic potential of copper oxide nanoparticles in human lung epithelial cells, Biochem. Biophys. Res. Commun. **396** (2010) 578–583, doi: https://doi.

org/10.1016/j.bbrc.2010.04.156.

66. *B. Fahmy, S. A. Cormier*, Copper oxide nanoparticles induce cytotoxicity and reactive oxygen species in airway epithelial cells, Toxicol. In Vitro **23** (2009) 1365–1371, doi: https://doi.org/10.1016/j.tiv.2009.08.005.
67. *S. Khalid, N. Afzal, J. A. Khan, Z. Hussain, A. S. Qureshi, H. Anwar, Y. Jamil*, Antioxidant resveratrol protects against copper oxide nanoparticle toxicity *in vivo*, Naunyn-Schmiedeberg's Arch. Pharmacol. **391** (2018) 1053–1062, doi: https://doi.org/10.1007/s00210-018-1526-0.
68. *A. S. Morsi, H. M. Ramadan, A. M. Youssef, N. A. Taha*, Curcumin nanoparticles attenuate copper nanoparticle-induced systemic toxicity in rats: a proof-of-concept study for a systemic protective strategy, Environ. Sci. Eur. **38** (2026) 84, doi: https://doi.org/10.1186/s12302-026-01379-8.
69. *A. Balasubramanyam, N. Sailaja, M. Mahboob, M. F. Rahman, S. Misra, S. M. Hussain, P. Grover*, Evaluation of genotoxic effects of oral exposure to aluminum oxide nanomaterials in rat bone marrow, Mutat. Res. **676** (2009) 41–47, doi: https://doi.org/10.1016/j.mrgentox.2009.03.004.
70. *B. S. Khangarot, R. S. Rathore, D. M. Tripathi*, Effects of chromium on humoral and cell-mediated immune responses and host resistance to disease in a freshwater catfish, Saccobranchus fossilis (Bloch), Ecotoxicol. Environ. Saf. **43** (1999) 11–20, doi: https://doi.org/10.1006/eesa.1998.1722.
71. *Y. Zhang, J. Luo, T. Zhu, Z. Yang, M. Jin, L. Jiao, Q. Zhou*, Excessive dietary Cr^{6+} had no adverse effect on mud crab (*Scylla paramamosain*) but provoke consumers health risk, Aquac. Rep. **27** (2022) 101397, doi: https://doi.org/10.1016/j.aqrep.2022.101397.
72. *H. Nabeshi, T. Yoshikawa, K. Matsuyama, Y. Nakazato, S. Tochigi, S. Kondoh, T. Hirai, T. Akase, K. Nagano, Y. Abe, Y. Yoshioka, H. Kamada, N. Itoh, S.-i. Tsunoda, Y. Tsutsumi*, Oral ingestion of hexavalent chromium through drinking water and cancer mortality in an industrial area of Greece – An ecological study, Environ. Health **10** (2011) 50, doi: https://doi.org/10.1186/1476-069X-10-50.
73. *G. Mekky, M. Seeds, A. E.-A. A. Diab, A. M. Shehata, O. A.-H. Ahmed-Farid, D. Alzebdeh, C. Bishop, A. Atala*, The potential toxic effects of magnesium oxide nanoparticles and valproate on liver tissue, J. Biochem. Mol. Toxicol. **35** (2021) e22676, doi: https://doi.org/10.1002/jbt.22676.
74. *Z. Wang, X. Zhang, G. Fan, Y. Que, F. Xue, Y. Liu*, Toxicity Effects and Mechanisms of MgO Nanoparticles on the Oomycete Pathogen Phytophthora infestans and Its Host Solanum tuberosum, Toxics **10** (2022) 553, doi: https://doi.org/10.3390/toxics10100553.
75. *E. Wigenstam, L. Elfsmark, A. Bucht, S. Jonasson*, Inhaled sulfur dioxide causes pulmonary and systemic inflammation leading to fibrotic respiratory disease in a rat model of chemical-induced lung injury, Toxicology **368–369** (2016) 28–36, doi: https://doi.org/10.1016/j.tox.2016.08.018.
76. *H. Shi, R. Magaye, V. Castranova, J. Zhao*, Titanium dioxide nanoparticles: A review of current toxicological data, Part. Fibre Toxicol. **10** (2013) 15, doi: https://doi.org/10.1186/1743-8977-10-15.
77. *J. Wang, G. Zhou, C. Chen, H. Yu, T. Wang, Y. Ma, G. Jia, Y. Gao, B. Li, J. Sun, Y. Li, F. Jiao, Y. Zhao, Z. Chai*, Acute toxicity and biodistribution of different sized titanium dioxide particles in mice after oral administration, Toxicol. Lett. **168** (2007) 176–185, doi: https://doi.org/10.1016/j.toxlet.2006.12.001.
78. *J. Shi, S. Han, J. Zhang, Y. Liu, Z. Chen, G. Jia*, Advances in genotoxicity of titanium dioxide nanoparticles *in vivo* and *in vitro*, NanoImpact **25** (2022) 100377, doi: https://doi.org/10.1016/j.impact.2021.100377.
79. *K. Yamashita, Y. Yoshioka, K. Higashisaka, K. Mimura, Y. Morishita, M. Nozaki, T. Yoshida, T. Ogura, H. Nabeshi, K. Nagano, Y. Abe, H. Kamada, Y. Monobe, T. Imazawa, H. Aoshima, K. Shishido, Y. Kawai, T. Mayumi, S.-i. Tsunoda, N. Itoh, T. Yoshikawa, I. Yanagihara, S. Saito, Y. Tsutsumi*, Silica and titanium dioxide nanoparticles cause pregnancy complications in mice, Nat. Nanotechnol. **6** (2011) 321–328, doi: https://doi.org/10.1038/nnano.2011.41.
80. *Z. Zhao, X.-S. Luo, Y. Jing, H. Li, Y. Pang, L. Wu, Q. Chen, L. Jin*, *In vitro* assessments of bioaccessibility and bioavailability of $PM_{2.5}$ trace metals in respiratory and digestive systems and their oxidative potential, J. Hazard. Mater. **409** (2021) 124638, doi: https://doi.org/10.1016/j.jhazmat.2020.124638.
81. *J. Khan, N. D. Kim, C. Bromhead, P. Truman, M. C. Kruger, B. L. Mallard*, Hepatotoxicity of Titanium Dioxide Nanoparticles, J. Appl. Toxicol. **45** (2025) 23–46, doi: https://doi.org/10.1002/jat.4626.
82. *Y. Yao, Y. Zang, J. Qu, M. Tang, T. Zhang*, The toxicity of metallic nanoparticles on liver: The subcellular damages, mechanisms, and outcomes, Int. J. Nanomed. **14** (2019) 8787–8804, doi: https://doi.org/10.2147/IJN.S212907.
83. *L. Arms, D. Smith, J. Flynn, W. Palmer, A. Martin, A. Woldu, S. Hua*, Advantages and limitations of current techniques for analyzing the biodistribution of nanoparticles, Front. Pharmacol. **9** (2018) 802, doi: https://doi.org/10.3389/fphar.2018.00802.
84. *Z. Ferdous, A. Nemmar*, Health impact of silver nanoparticles: A review of the biodistribution and toxicity following various routes of exposure, Int. J. Mol. Sci. **21** (2020) 2375, doi: https://doi.org/10.3390/ijms21072375.
85. *I. Y. Adamson, D. H. Bowden*, Crocidolite-induced pulmonary fibrosis in mice: Cytokinetic and biochemical studies, Am. J. Pathol. **122** (1986) 261–267, PMID: 3004226.
86. *B. T. Mossman, A. Churg*, Mechanisms in the pathogenesis of asbestosis and silicosis, Am. J. Respir. Crit. Care Med. **157** (1998) 1666–1680, doi: https://doi.org/10.1164/ajrccm.157.5.9707141.
87. *C. Gong, G. Tao, L. Yang, J. Liu, H. He, Z. Zhuang*, The role of reactive oxygen species in silicon dioxide nanoparticle-induced cytotoxicity and DNA damage in HaCaT cells, Mol. Biol. Rep. **39** (2012) 4915–4925, doi: https://doi.org/10.1007/s11033-011-1287-z.
88. *R. F. Hamilton, M. C. Buford, M. B. Wood, B. Arnone, M. Morandi, A. Holian*, Engineered carbon nanoparticles alter macrophage immune function and initiate airway hyper-responsiveness in the BALB/c mouse model, Nanotoxicology **1** (2007) 104–117, doi: https://doi.org/10.1080/17435390600926939.
89. *Y. Xuan, W. Zhang, X. Zhu, S. Zhang*, An updated overview of some factors that influence the biological effects of nanoparticles, Front. Bioeng. Biotechnol. **11** (2023) 1254861, doi: https://doi.org/10.3389/fbioe.2023.1254861.
90. *N. H. A. Nguyen, P. Falagan-Lotsch*, Mechanistic insights into the biological effects of engineered nanomaterials: A focus on gold nanoparticles, Int. J. Mol. Sci. **24** (2023) 4109, doi: https://doi.org/10.3390/ijms24044109.
91. *S. L. Easo, P. V. Mohanan*, *In vitro* hematological and *in vivo* immunotoxicity assessment of dextran stabilized iron oxide nanoparticles, Colloids Surf. B **134** (2015) 122–130, doi: https://doi.org/10.1016/j.colsurfb.2015.06.046.
92. *M. Mahmoudi, S. Sant, B. Wang, S. Laurent, T. Sen*, Superparamagnetic iron oxide nanoparticles (SPIONs): Development, surface modification and applications in chemotherapy, Adv. Drug Deliv. Rev. **63** (2011) 24–46, doi: https://doi.org/10.1016/j.addr.2010.05.006.

93. *L. Bregoli, F. Chiarini, A. Gambarelli, G. Sighinolfi, A. M. Gatti, P. Santi, A. M. Martelli, L. Cocco*, Toxicity of antimony trioxide nanoparticles on human hematopoietic progenitor cells and comparison to cell lines, Toxicology **262** (2009) 121–129, doi: https://doi.org/10.1016/j.tox.2009.05.017.
94. *E. A. Huber, J. M. Cerreta*, Mechanisms of cell injury induced by inhaled molybdenum trioxide nanoparticles in Golden Syrian hamsters, Exp. Biol. Med. **247** (2022) 2067–2080, doi: https://doi.org/10.1177/15353702221104033.
95. *A. Fakhri, P. Afshar Nejad*, Antimicrobial, antioxidant and cytotoxic effect of molybdenum trioxide nanoparticles and application for degradation of ketamine under different light illumination, J. Photochem. Photobiol. B: Biol. **159** (2016) 211–217, doi: https://doi.org/10.1016/j.jphotobiol.2016.04.002.
96. *P. Jalili, S. Huet, R. Lanceleur, G. Jarry, L. Le Hegarat, F. Nesslany, K. Hogeveen, V. Fessard*, Genotoxicity of aluminum and aluminum oxide nanomaterials in rats following oral exposure, Nanomaterials **10** (2020) 305, doi: https://doi.org/10.3390/nano10020305.
97. *O. Bondarenko, K. Juganson, A. Ivask, K. Kasemets, M. Mortimer, A. Kahru*, Toxicity of Ag, CuO and ZnO nanoparticles to environmentally relevant test organisms and mammalian cells in vitro: A critical review, Arch. Toxicol. **87** (2013) 1181–1200, doi: https://doi.org/10.1007/s00204-013-1079-4.
98. *R. J. Graham, H. Bhatia, S. Yoon*, Consequences of trace metal variability and supplementation on Chinese hamster ovary (CHO) cell culture performance: A review of key mechanisms and considerations, Biotechnol. Bioeng. **116** (2019) 3446–3456, doi: https://doi.org/10.1002/bit.27140.
99. *C. Y. Tang, Z. Yang*, Chapter 8 – Transmission electron microscopy (TEM), in: Membrane Characterization, Elsevier, 2017, pp. 145–159, doi: https://doi.org/10.1016/B978-0-444-63776-5.00008-5.
100. *N. Kaur*, Transmission electron microscopy: A powerful and novel scientific technique with nanoscale resolution, in: Microscopic Techniques for the Non-Expert, Springer, Cham, 2022, doi: https://doi.org/10.1007/978-3-030-99542-3_9.
101. *B. J. Inkson*, 2 – Scanning electron microscopy (SEM) and transmission electron microscopy (TEM) for materials characterization, in: Materials Characterisation Using Nondestructive Evaluation Methods, Elsevier, 2016, pp. 17–43, doi: https://doi.org/10.1016/B978-0-08-100040-3.00002-X.
102. *M. Malatesta*, Transmission electron microscopy as a powerful tool to investigate the interaction of nanoparticles with subcellular structures, Int. J. Mol. Sci. **22** (2021) 12789, doi: https://doi.org/10.3390/ijms222312789.
103. *D. Birant*, Comparison of decision tree algorithms for predicting potential air pollutant emissions with data mining models, J. Environ. Inform. **17** (2011) 46-53, doi: https://doi.org/10.3808/jei.201100186.
104. *W. Shi, W. Zeng*, Application of k-means clustering to environmental risk zoning of a chemical industrial area, Front. Environ. Sci. Eng. **8** (2014) 117–127, doi: https://doi.org/10.1007/s11783-013-0581-5.
105. *K. Szramowiat-Sala*, Artificial intelligence in environmental monitoring: Application of artificial neural networks and machine learning for pollution prevention and toxicity measurements, Preprints (2023) 2023071298, doi: https://doi.org/10.20944/preprints202307.1298.v1.
106. *F. Gagné, C. Blaise*, Predicting the toxicity of complex mixtures using artificial neural networks, Chemosphere **35** (1997) 1343–1363, doi: https://doi.org/10.1016/S0045-6535(97)00178-1.
107. *T. Oral, M. Ensari Özay, R. Uçan, D. Aker, E. Can, B. Altınten*, Measurement and Evaluation of Dust Concentrations in the Air After the Kahramanmaraş Earthquake in Turkey, Int. J. Environ. Res. Public Health **22** (2025) 649, doi: https://doi.org/10.3390/ijerph22040649.
108. *F. Eryilmaz, M. Güzel, M.U. Şimşek, İ. Kök, S. Özdemir*, The impact of earthquakes on air pollution: Machine learning-based air quality analysis following the Kahramanmaraş earthquakes, 2024 Mediterranean Smart Cities Conference (MSCC), Martil – Tetuan, Morocco, 2024, pp. 1–6, doi: https://doi.org/10.1109/MSCC62288.2024.10697006.
109. *G. G. Kabito, Y. Tefera, C. Ramkissoon, S. Gaskin*, Evidence-based dust exposure prediction and/or control tools in occupational settings: A scoping review protocol, PLoS One **19** (2024) e0309967, doi: https://doi.org/10.1371/journal.pone.0309967.
110. *R. B. Hamanaka, G. M. Mutlu*, Particulate matter air pollution: effects on the respiratory system, J. Clin. Invest. **135** (2025) e194312, doi: https://doi.org/10.1172/JCI194312.
111. *A. N. Pavlyuchenkova, N. V. Vorobjeva, A. I. Ivaneev, M. S. Ermolin, P. S. Fedotov, R. A. Zinovkin, M. A. Chelombitko, B. V. Chernyak*, Urban dust nanoparticles drive inflammatory activation of human neutrophils and macrophages *in vitro*, Environ. Sci. Pollut. Res. **32** (2025) 26541–26553, doi: https://doi.org/10.1007/s11356-025-37172-y.
112. *F. Ustaoğlu, M. M. Yazman, N. Batan, B. Yüksel*, Disaster-induced toxic metal mobilization in post-earthquake street dust of Adıyaman, Türkiye: Pollution indices, receptor model source apportionment, and probabilistic health risk evaluation, J. Hazard. Mater. **506** (2026) 141606, doi: https://doi.org/10.1016/j.jhazmat.2026.141606.
113. *A. Zanoletti, E. Bontempi*, The impacts of earthquakes on air pollution and strategies for mitigation: a case study of Turkey, Environ. Sci. Pollut. Res. **31** (2024) 24662–24672, doi: https://doi.org/10.1007/s11356-024-32592-8.
114. *R. Manzueta, P. Kumar, A. H. Ariño, C. Martín-Gómez*, Strategies to reduce air pollution emissions from urban residential buildings, Sci. Total Environ. **951** (2024) 175809, doi: https://doi.org/10.1016/j.scitotenv.2024.175809.

SAŽETAK

Eksperimentalno i računalno modeliranje imunološkog odgovora te tokisikološka procjena urbanih nanočestica u gradu pogođenom potresom

Yakup Ermurat [a,b*]

Urbane nanočestice (UNP) nastale u okolišu nakon katastrofa predstavljaju složenu i potencijalno opasnu sastavnicu urbanog onečišćenja sa značajnim posljedicama za javno zdravlje. U ovom su istraživanju ispitane fizikalno-kemijske značajke i potencijalni biološki učinci urbanih nanočestica prikupljenih u središtu grada Kahramanmaraşa u Turskoj, pogođenog potresima u veljači 2023. godine. Uzorci prašine analizirani su transmisijskom elektronskom mikroskopijom (TEM), kojom je utvrđena heterogena populacija čestica veličine od 50 do 500 nm, uključujući značajan udio ultrafinih čestica (< 100 nm) nepravilne i aglomerirane morfologije. Energetski disperzivnom rendgenskom spektroskopijom (EDX) utvrđeni su dominantni elementi (O, C, Ca, Si), uz prijelazne metale poput Fe, Cr i Cu, što upućuje na različite izvore urbanih nanočestica. Računalne analize pokazale su značajnu varijabilnost sastava i međusobne odnose pojedinih elemenata. Za procjenu potencijalnih toksikoloških i imunoloških učinaka primijenjeni su prediktivni modeli. Modeli strojnog učenja pokazali su da na toksičnost utječu veličina čestica, elementni sastav i trajanje izloženosti, pri čemu su se krom i bakar izdvojili kao ključni čimbenici povezani s oksidacijskim stresom. Simulacije Markovljevim lancima i Monte Carlo metodom dodatno su ukazale na dinamičko ponašanje čestica, potencijal bioakumulacije i povezane nesigurnosti tijekom vremena. Integriranjem strukturnih, sastavnih i računalnih rezultata dobiven je sveobuhvatan okvir za razumijevanje rizika povezanih s nanočesticama. Usporedba s eksperimentalnim istraživanjima provedenima *in vivo* ili *in vitro* upućuje na moguće učinke koji uključuju oksidacijski stres, upalne procese i poremećaj regulacije imunološkog sustava. Dobiveni rezultati naglašavaju važnost multidisciplinarnog pristupa procjeni zdravstvenih rizika povezanih s okolišem u urbanim područjima nakon potresa.

Ključne riječi
Urbane nanočestice, eksperimentalno i računalno modeliranje, transmisijska elektronska mikroskopija (TEM), imunološki odgovor, nanotoksikološki učinci

[a] *Department of Basic Sciences, Engineering Architecture and Design Faculty, Kahramanmaraş İstiklal University, 46 060 Kahramanmaraş, Turska*
[b] *Engineering Faculty, Bolu Abant Izzet Baysal University, 14 030 Bolu, Turska*

Izvorni znanstveni rad
Prispjelo 25. veljače 2026.
Prihvaćeno 3. svibnja 2026.